JOURNAL OF PROPULSION AND POWER
Vol. 11, No. 4, July–August 1995

Intrinsic Combustion Instability of Solid Energetic Materials

L. DeLuca,* R. Di Silvestro,† and F. Cozzi‡
Politecnico di Milano, 20133 Milano, Italy

In the first part, a review is offered of the intrinsic stability of pressure- or radiation-driven burning of solid propellants with chemically inert condensed phase. The two main approaches today available [flame modeling and the Zeldovich–Novozhilov (ZN) method] are both considered. Within the current quasi-steady homogeneous one-dimensional framework, the intrinsic burning stability boundaries and frequency of the self-sustained oscillatory solution predicted by several techniques are the same; the classical boundaries predicted by the ZN are somewhat extended. The intrinsic stability boundaries for pressure-driven or radiation-driven burning are identical in the limit of fully opaque condensed phase (surface absorption). However, the burning configurations are affected by the impinging radiant flux. Some peculiar effects of radiation assisted burning are illustrated. In the second part of this article, an extension is presented to chemical reactions volumetrically distributed in the condensed phase with a uniform heat release rate distribution. Frequency response functions and unbounded response limits are obtained; both recover the particular configuration of chemically inert condensed phase.

Nomenclature

A = nondimensional function, Eq. (31); Denison and Baum nondimensional parameter, Eq. (53); Krier–T'ien–Sirignano–Summerfield transient flame mode nondimensional parameter, Eq. (54)
$\tilde{A}_s$ = nondimensional function, Eq. (6)
a = nondimensional function defined by Eq. (13)
$\bar{\bar{a}}_\lambda$ = average volumetric absorption coefficient, cm^{-1}
B = nondimensional function introduced by Culick, Eq. (39); Krier–T'ien–Sirignano–Summerfield transient flame mode nondimensional parameter, Eq. (53)
B_p = nondimensional function, Eq. (37)
B_q = nondimensional function, Eq. (45)
$\tilde{B}_s$ = nondimensional function, Eq. (7)
b = nondimensional function, Eq. (14)
C_1 = nondimensional function, Eq. (36)
C_3 = nondimensional function, Eq. (36)
C_6 = nondimensional function, Eq. (36)
c = specific heat, cal/g K
D_1 = $(\alpha_c/\bar{r}_b)\lfloor d\bar{T}/dx\rfloor_{x=0^-}/(\bar{T}_s - T_1)$, nondimensional function
D_2 = $(\alpha_c/\bar{r}_b)^2\lfloor d^2\bar{T}/dx^2\rfloor_{x=0^-}/(\bar{T}_s - T_1)$, nondimensional function
D_3 = $\dfrac{(D^+ - D^-)\exp[\bar{r}_b/\alpha_c(\lambda_2 - \lambda_1)\bar{l}_c]}{\lambda_2 - \lambda_1 - D^+ + D^-}$, nondimensional function
D_4 = $\dfrac{\dfrac{D^+}{\iota_r^2 - \iota_r + \lambda_1\lambda_2} - \dfrac{D^-}{\iota_r^2 - \iota_r + \lambda_1\lambda_2}}{\lambda_2 - \lambda_1 - D^+ + D^-}\exp\left(\dfrac{\bar{r}_b}{\alpha_c}\lambda_2\bar{l}_c\right)$, nondimensional function
D_{30} = $-\dfrac{D^+ - D^-}{1 + D^+ - D^-}\exp\left(-\dfrac{\bar{r}_b}{\alpha_c}\bar{l}_c\right)$, nondimensional function
D_{31} = $-D_{30}\left(\dfrac{\bar{r}_b}{\alpha_c}\bar{l}_c + \dfrac{1}{1 + D^+ - D^-}\right)$, nondimensional function
$D^\pm$ = $\dfrac{\alpha_c}{\bar{r}_b}\dfrac{\lfloor d^2\bar{T}/dx^2\rfloor_{x=-l_c^\pm}}{\lfloor d\bar{T}/dx\rfloor_{x=-l_c}}$, nondimensional function
$E_{(\,)}$ = $\bar{E}_{(\,)}/\bar{\mathcal{R}}/T_{(\,)}$, nondimensional activation energy
$\bar{E}_{(\,)}$ = activation energy, cal/mole
$f(p)$ = function, Eq. (30)
$g(\ldots)$ = function defining temperature dependence of characteristic time parameter
$H_{(\,)}$ = $Q_{(\,)}/[c_{\mathrm{ref}}(\bar{T}_s - T_{\mathrm{ref}})]$, nondimensional heat release
I_0 = external radiant flux intensity, cal/cm^2 s
i = imaginary unit
K = nondimensional function, Eq. (49)
k = ZN parameter, Eq. (19)
$k_{(\,)}$ = thermal conductivity, cal/cm s K
l = length, cm
l_c = thickness of condensed phase chemically reacting layer, cm
$\bar{\bar{M}}$ = average molecular mass of product gas mixture, g/mole
m = mass burning rate, g/cm^2 s
N_t = radiation fraction absorbed below reacting surface layer, Eq. (5)
n = pressure exponent of steady-state burning rate law
n_s = pressure exponent of surface pyrolysis law, Eq. (6) or Eq. (7)
p = pressure, atm
p_{ref} = 68 atm, reference pressure, atm
Q = heat release, cal/g (positive if exothermic)
Q_{ref} = $c_{\mathrm{ref}}(T_{s,\mathrm{ref}} - T_{\mathrm{ref}})$, reference heat release, cal/g
Q_x = total (surface-concentrated Q_s + volume-distributed Q_c) condensed phase heat release, cal/g
q = $\tilde{q}/[\rho_c c_{\mathrm{ref}} r_{b,\mathrm{ref}}(T_{s,\mathrm{ref}} - T_{\mathrm{ref}})]$, nondimensional reference energy flux; Denison and Baum nondimensional parameter, Eq. (54)
$\tilde{q}$ = energy flux intensity, cal/cm^2 s
q_r = $I_0/[\rho_c c_{\mathrm{ref}}\bar{r}_b(\bar{T}_s - T_{\mathrm{ref}})]$, nondimensional external radiant flux

Received Aug. 13, 1994; revision received March 2, 1995; accepted for publication March 2, 1995.

*Professor, Dipartimento di Energetica, 32 Piazza Leonardo da Vinci.
†M.S. Candidate, Dipartimento di Energetica, 32 Piazza Leonardo da Vinci.
‡Doctoral Candidate, Dipartimento di Energetica, 32 Piazza Leonardo da Vinci.

q_{ref} = $\rho_c c_{ref} r_{b,ref}(T_{s,ref} - T_{ref})$, reference energy flux, cal/cm² s
R = nondimensional reference burning rate
R_p = mass burning rate response to pressure fluctuations, Eq. (26)
R_q = mass burning rate response to radiation fluctuations, Eq. (26)
$\mathcal{R}$ = universal gas constant; 1.987 cal/mole K or 82.1 atm cm³/mole K
r = ZN parameter defined in Eq. (19)
r_b = burning rate, cm/s
$r_{b,ref}$ = $r_b(p_{ref})$, reference burning rate, cm/s
$\bar{r}_\lambda$ = average reflectivity of burning surface, cm^{-1}
T = temperature, K
T_{ref} = 300 K, reference temperature
$T_{s,ref}$ = $T_s(p_{ref})$, reference surface temperature
T_1 = initial propellant temperature, K
t = time coordinate
$t^\dagger$ = $t(c_g/k_g)\langle\rho_g\rangle$, characteristic time parameter, g/cm² s^{-2}
$\tilde{u}$ = temperature disturbance, K
W_p = nondimensional function introduced by Culick, Eq. (40)
$W_p(\gamma)$ = nondimensional function, Eq. (38)
w_s = power of Krier–T'ien–Sirignano–Summerfield transient flame mode pyrolysis law, Eq. (7)
x = space coordinate, cm
α = thermal diffusivity, cm²/s; exponent of temperature dependence of chemical reaction rates; Denison and Baum nondimensional parameter, Eq. (53)
β = overall reaction order of chemical reactions
γ = flame elongation parameter for distributed flames, Eq. (27) and Eq. (28)
δ = ZN parameter, Eq. (20)
$\delta(\ldots)$ = Dirac-delta function
δ_q = ZN parameter, Eq. (46)
$\tilde{\varepsilon}$ = chemical reaction rate, 1/s
ζ = $mc_g/k_g x$, nondimensional group
ι_r = $\bar{a}_\lambda \cdot \alpha_c/\bar{r}_b$, nondimensional ratio of conductive to radiant layer thickness
Λ_1 = nondimensional function, Eq. (60)
Λ_3 = nondimensional function, Eq. (65)
Λ_{10} = $1/(1 + D_{30})$, nondimensional function
Λ_{11} = $\dfrac{1}{1 + D_{30}}\left[1 - D_{30} - \dfrac{D_{31}}{1 + D_{30}}\right]$, nondimensional function
$\lambda_{1,2}$ = $(1 \pm \sqrt{1 + 4i\Omega})/2$, complex characteristic roots of fluctuating thermal profile
μ = ZN parameter, Eq. (18)
μ_q = ZN parameter, Eq. (24)
ν = ZN parameter, Eq. (18); frequency, Hz
ν_q = ZN parameter, Eq. (24)
ρ = density, g/cm³
Φ = phase
Ω = $\omega \cdot \alpha_c/\bar{r}_b^2$, nondimensional circular frequency
ω = $2\pi\nu$, circular frequency, rad/s
$-\infty$ = far upstream
$+\infty$ = far downstream
$\langle\ \rangle$ = space-averaged value

Subscripts
c = condensed phase
c, s = burning surface, condensed phase side
f = flame
g = gas phase
g, s = burning surface, gas phase side
l_c = edge of condensed phase chemical reacting layer
p = pressure
q = radiation
ref = reference
s = burning surface
λ = spectral value
0 = at the burning surface; initial value in time
1 = cold boundary value

Superscripts
$'$ = fluctuating value
$\bar{}$ = steady-state value
$=$ = value averaged over chemical composition
$\tilde{}$ = dimensional value

I. Introduction

A LARGE number of models for steady and/or unsteady combustion of solid rocket propellants has been proposed by investigators in several countries. Over the years a common stronghold has emerged, along different guidelines, first in Russia (known as Zeldovich–Novozhilov or ZN method[1,2] and, later, in the U.S. and Western countries (known as flame modeling or FM method). Both approaches intend to evaluate the transient energy feedback to the burning surface from the adjacent gas phase: the FM method by solving gas phase conservation equations, the ZN method by performing steady-state experiments with parametrically variable initial temperature. Although drastically different, the two methods share the basic assumptions of a one-dimensional strand of homogeneous solid propellant burning with a quasi-steady gas phase [quasi-steady homogeneous one-dimensional (QSHOD framework)]. Currently, this strategy is still the most accepted in dealing with solid propellant burning. It is recognized, however, that the limitations of this by now classical approach are severe.

Solid-propellant burning assisted by external radiation is today an area of renewed interest for both practical applications and fundamental knowledge. In particular, no combustion theory is today accurate enough to predict the frequency response data required by the current procedures to test the combustion stability of solid rocket motors.[3] Furthermore, the experimental techniques usually implemented are money- and time-consuming.[4] These experimental tools try to produce data by directly perturbing the pressure field. The suggestion was made[5] of using a radiation source as perturbing energy input. However, radiation-assisted burning yields problems of radiation interactions with reactive media not yet fully understood. The related intrinsic combustion stability features some unexpected behavior even within the familiar QSHOD framework. An excellent background to radiation-driven burning was offered by Ibiricu and Williams,[6] using high activation energy asymptotics and formalizing the equivalence principle.

An important objective of any transient flame modeling would be to relax the quasisteady gas phase assumption, which restricts applications to a frequency range from 0 to some 1000 Hz. Several contributions are available.[7–16] T'ien[7] and Novozhilov[9] published papers based on the time lag concept first introduced in liquid rocket propulsion. Margolis and Williams[14,15] went well beyond the classical QSHOD limitations by relaxing, for large values of activation energies for both surface pyrolysis and gas phase processes, the assumptions of quasisteadiness as well as quasiplanarity of the gas phase and allowing two-phase flow. Further work is reported in the FM framework by Clavin and Lazimi (pressure-driven frequency response function of sharp flames[16]), and in the ZN framework by Novozhilov.[8–13]

The purpose of this article is to 1) review the present status of intrinsic stability for both pressure- and radiation-driven combustion of solid propellants with chemically inert condensed phase; and 2) to somewhat extend the treatment to solid propellants with chemically reacting condensed phase. The QSHOD framework is accepted. Although attention is focused on solid rocket propellants, most developments more broadly concern solid energetic materials.

Linear stability analyses for pressure perturbations were first presented by Denison and Baum[17] for a sharp flame and Novozhilov[8,13] by the ZN method. A systematic investigation was carried out by Culick for a variety of flame configurations[18–21]; further work was performed, among others, by Krier et al.[22] and T'ien[23] for distributed flames. Stability analyses for external radiation perturbations were carried out by the ZN method solely.[24–28] Few papers dealt with chemical reactions distributed in the condensed phase: results were presented[18,29] for pressure-driven burning.

II. Formulation of the QSHOD Problem

The basic set of governing equations and physical assumptions of the broad QSHOD framework is discussed. All developments assume a one-dimensional strand of homogeneous solid propellant burning with a quasisteady gas phase subjected to pressure and/or (external) radiant flux changes in time. Thermophysical properties are at most only pressure-dependent. The FM method mainly is described, but is supplemented where needed with the alternative ZN method.[1,2,8,13]

Consider a strand of solid propellant burning, with no velocity coupling, in a vessel at uniform pressure and possibly subjected to a collimated radiant flux originated exclusively from a continuous external source of thermal nature. Overall, assume one-dimensional processes, no radiation scattering, no photochemistry, and no external forces. Define a Cartesian x axis with its origin anchored at the burning surface and positive in the gas-phase direction.

A. Condensed Phase Assumptions and Governing Equations

Let the condensed phase be a semi-infinite slab of uniform and isotropic composition, chemically inert, with constant thermophysical properties, and $T_1 = T_{\text{ref}}$. The energy equation in the condensed phase ($x < 0$) is

$$\frac{\partial T}{\partial t} + r_b \frac{\partial T}{\partial x} = \alpha_c \frac{\partial^2 T}{\partial x^2} + N_t \frac{\bar{\tilde{a}}_\lambda}{\rho_c c_c}(1 - \bar{\tilde{r}}_\lambda) I_0 \exp(\bar{\tilde{a}}_\lambda x) \tag{1}$$

$$T(x, t = 0) = T_0(x < 0) \tag{2}$$

$$T(x \to -\infty, t) = T_1 \tag{3}$$

$$\tilde{q}_{c,s} = \tilde{q}_{g,s} + \rho_c r_b Q_s + (1 - N_t)(1 - \bar{\tilde{r}}_\lambda) I_0 \tag{4}$$

where at $x = 0$

$$\tilde{q}_{c,s} \equiv \left(k_c \frac{\partial T}{\partial x}\right)_{c,s}, \qquad \tilde{q}_{g,s} \equiv \left(k_g \frac{\partial T}{\partial x}\right)_{g,s}$$
$$N_t = \exp\left(-\bar{\tilde{a}}_\lambda \frac{\alpha_c}{\tilde{r}_b} \frac{\mathcal{R}\tilde{T}_s}{\tilde{E}_s}\right) \tag{5}$$

The boundary condition of Eq. (4), needed to evaluate the condensed phase thermal gradient, is where FM and ZN approaches differ. While FM needs in particular an explicit formulation of the heat feedback $\tilde{q}_{g,s}$, ZN resorts to a suitable experimental steady-state data-set. Details of the burning surface and gas phase are not requested by ZN. The N_t estimate was suggested by Son et al.[30]

B. Burning Surface Assumptions and Governing Equations

Let the burning surface be an infinitesimally thin planar surface subjected to one-step, irreversible gasification process. Both pyrolysis laws accepted in the literature for concentrated surface gasification are implemented: the standard Arrhenius exponential law

$$m_s(p, T_s) = \tilde{A}_s p^{n_s} T_s^{\alpha_s} \exp[-(\tilde{E}_s/\mathcal{R}T_s)] \tag{6}$$

and the alternative Krier–T'ien–Sirignano–Summerfield transient flame model (KTSS) power law[22]:

$$m_s(p, T_s) = \tilde{B}_s p^{n_s} T_s^{\alpha_s} (T_s - T_1)^{w_s} \tag{7}$$

Notice that analysis of the intrinsic burning stability in the broad QSHOD framework does not require formulating a specific pyrolysis law as long as the surface mass production is bounded and monotonic, as indeed observed.

The (net) heat release of gasification reactions concentrated at the burning surface is computed as

$$Q_s(p, T_s) = Q_s(\bar{p}) + (c_g - c_c)(\tilde{T}_s - T_s) \tag{8}$$

where the dependence $Q_s(\bar{p})$ is experimentally deduced under steady-state operations.

C. Gas-Phase Assumptions and Governing Equations

Let the gas-phase mixture be a semi-infinite column of thermally perfect components with no interactions with radiation. The flow is assumed to be one-phase, laminar, nonviscous, low-subsonic, and with Lewis number = 1. Thus, for all quasisteady flames, the first energy integral yields the heat feedback to the burning surface from the gas phase ($x > 0$) as

$$\tilde{q}_{g,s}(p, m) = \int_{0+}^{x_{f-}} Q_g \rho_g \tilde{\varepsilon}_g \exp(-\zeta)\, dx \tag{9}$$

implying that the thermal gradient at the edge of the flame is much less than at the burning surface.[31,32] The quantity $\zeta \equiv mc_g/k_g x$ is a convenient nondimensional position. In the spirit of quasisteady gas phase, the energy release $Q_g(p)$ in the gas phase is defined once for all by an integral energy balance carried out, under steady-state operations, from the burning surface to the flame end

$$Q_g(\bar{p}) + Q_s(\bar{p}) \equiv Q(\bar{p}) = c_c(\tilde{T}_s - T_1) + c_g(\tilde{T}_f - \tilde{T}_s) \tag{10}$$

For quantitative trends the previous formal result for heat feedback requires modeling of the spatial heat release rate. But analysis of the intrinsic burning stability in the broad QSHOD framework does not require formulating a specific flame model as long as the heat feedback is bounded and unimodal, as indeed observed.

III. Nonlinear Approach to FM Intrinsic Burning Stability

The problem of finding the stability and instability regions of the steady-state regime, under general perturbations of the initial thermal profile, can be treated by suitably reformulating the QSHOD problem under examination as an initial value problem for an abstract nonlinear parabolic equation in an infinite-dimensional normed functional space (Banach space) consisting of thermal profiles. Let us assume that the initial thermal profile $T_0(x)$ deviates from the pertaining time-invariant steady profile by a small but finite disturbance, in such a way that

$$T_0(x) = \tilde{T}(x) + \tilde{u}_0(x) \tag{11}$$

The purpose of the study is to investigate the long-time asymptotic behavior of $\tilde{u}(x, t)$. The main tool in the analysis is a generalized version of the well-known principle of linearized stability for semilinear parabolic equations.[33,34] This general approach is valid for all quasisteady gas phase thermal flames featuring mathematically smooth (up to the second derivative) functions for the surface pyrolysis (assumed bounded and increasing) and heat feedback law (assumed bounded and unimodal). All commonly used transient flame models, including the premixed flame by Denison and Baum[17] and the distributed flame by KTSS[22] are recovered as particular cases.

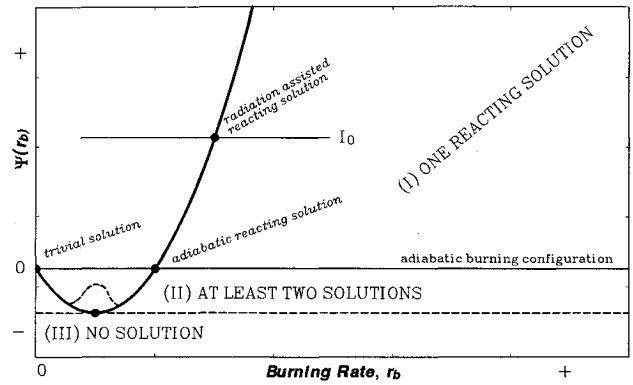

Fig. 1 Existence and uniqueness of time-invariant steady-state solution.

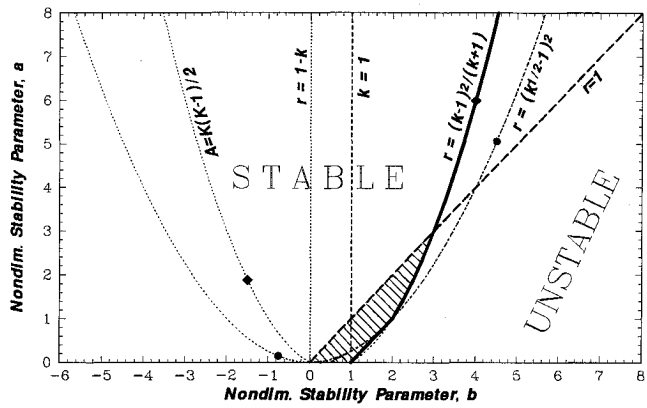

Fig. 2 QSHOD FM or ZN intrinsic stability map for pressure or surface radiation-driven burning. Solid line is the QSHOD FM intrinsic stability boundary.

The surface boundary condition of Eq. (4), under steady operating conditions and for surface absorption (i.e., fully opaque condensed phase: $N_t = 0$), can be rewritten as

$$\Psi(\bar{r}_b) = (1 - \bar{\bar{r}}_\lambda)\bar{I}_0 \tag{12}$$

Thus, with reference to the sketch in Fig. 1, it can be shown[35] that the QSHOD problem of Eqs. (1–10) admits 1) a unique time-invariant steady-state nontrivial solution corresponding to $\bar{r}_b > 0$ if the propellant sample is subjected to a positive (incoming) heat flux; 2) two solutions, $\bar{r}_b = 0$ and $\bar{r}_b > 0$, under adiabatic burning; 3) at least two nontrivial solutions, $\bar{r}_{b,1} > 0$ and $\bar{r}_{b,2} > 0$, if the propellant sample is subjected to a moderate negative (outgoing) heat flux; 4) no solution at all if the negative heat flux is too large.

Let us now consider[35] a pressure-driven or radiation-driven burning regime in the limit of surface absorption. Under the above circumstances, the problem has exactly one nontrivial time-invariant steady-state solution. The stability of such a solution is then studied by assuming a perturbation of the time-invariant steady profile as initial datum and then investigating its asymptotic behavior in time. The admissible perturbations must be "sufficiently" small (in a mathematical sense) for any $x \leq 0$ and exponentially decaying for $x \to -\infty$.

The mathematical analysis reveals the convenience of collecting the relevant ballistic properties under two nondimensional variables, defined, respectively, in terms of burning surface and gas-phase properties:

$$a \equiv \left[(T_s - T_1)\frac{\partial \ell_n m_s}{\partial T_s}\right]_{\bar{T}_s} \tag{13}$$

$$b \equiv \left[\left(\frac{\partial \tilde{q}_{g,s}}{\partial m_s} + Q_s\right)\frac{\partial \ell_n m_s}{\partial T_s}\right]_{\bar{T}_s} - \frac{c_g - c_c}{c_c} \tag{14}$$

Notice that a is positive, while b can be of arbitrary sign. Notice also that these parameters implicitly depend on the radiant flux intensity as well. With reference to Fig. 2, the intrinsic burning stability condition for small but finite size disturbances is determined as

$$b < 1 \quad \text{always stable} \tag{15}$$

$$b > 1 \quad \text{stable if} \quad a > \max[b - 1, (b/2)(b - 1)] \tag{16}$$

Thus, the stability boundary consists of the segment ($a = b - 1$:$1 < b < 2$), whose points would probably yield steady but nonplanar structures in a multidimensional analysis (steady bifurcation), and the arc of parabola [$a = b(b - 1)/2$:$b > 2$], whose points correspond to oscillatory solutions. The complementary region corresponds to instability of the time-invariant steady solution. The frequency of the oscillatory solution just at the stability boundary is given by

$$\Omega = [(b - 1)/2]\sqrt{b(b - 2)} \tag{17}$$

requiring $b > 2$ for real Ω.

For radiation-driven frequency response with volumetric absorption ($N_t \neq 0$ and ι_r = finite), a detailed mathematical analysis is in progress.[36] Although the limiting configuration of a very transparent condensed phase ($\iota_r << 1$) is recovered, the general treatment appears rather involved; further comments follow.

IV. ZN Intrinsic Burning Stability

For the reader's convenience, the classical ZN intrinsic stability analysis for pressure-driven burning is quickly revisited. In the original ZN formulation[13] four nondimensional parameters were introduced to describe the dependence of ballistic properties on pressure

$$\nu \equiv \left(\frac{\partial \ell_n \bar{m}}{\partial \ell_n \bar{p}}\right)_{T_1} \quad \text{and} \quad \mu \equiv \frac{1}{(\bar{T}_s - T_1)}\left(\frac{\partial \bar{T}_s}{\partial \ell_n \bar{p}}\right)_{T_1} \tag{18}$$

and ambient temperature

$$k \equiv (\bar{T}_s - T_1)\left[\frac{\partial \ell_n \bar{m}}{\partial T_1}\right]_p \quad \text{and} \quad r \equiv \left[\frac{\partial \bar{T}_s}{\partial T_1}\right]_p \tag{19}$$

A possible correlation among the four parameters is revealed by the Jacobian

$$\delta \equiv \frac{\partial(\ell_n \bar{m}, \bar{T}_s)}{\partial(\ell_n p, T_1)} = \nu r - \mu k \tag{20}$$

when $\delta = 0$, one of the four parameters can be evaluated from the remaining three.

The intrinsic stability of a steady-state regime is investigated by overlapping small perturbations, assumed of exponential nature in a complex frequency, to the steady-state solution and investigating their behavior in time. The domains for which $k > 0$ and $0 < r < 1$ are considered. The stability condition for a steady-state burning propellant is formulated as

$$k < 1 \quad \text{always stable} \tag{21}$$

$$k > 1 \quad \text{stable if} \quad r > \frac{(k - 1)^2}{k + 1} \tag{22}$$

This stability condition does not allow investigation of the asymptotic behavior of the perturbations far from the stability boundary. The natural oscillatory frequency just at the stability boundary is

$$\Omega = \frac{\sqrt{k}}{r} = \sqrt{k}\,\frac{(k+1)}{(k-1)^2} \tag{23}$$

being $\Omega \equiv \omega\alpha_c/\bar{r}_b^2$ a nondimensional frequency. Novozhilov (e.g., see p. 623 of Ref. 13) showed the exact equivalence of his results with those obtained by Denison and Baum[17] in the FM framework.

For radiation-driven burning, the mathematical analysis becomes more involved. Exactly the same formal results are obtained if surface absorption is assumed for the radiation-driven burning regime[27]; but relevant parameters implicitly depend on the radiant flux intensity as well. Thus, for pressure-driven or radiation-driven burning in the limit of surface absorption, the same set of equations holds true [Eqs. (19–23)] if a straightforward generalization of the definitions in Eq. (18) is performed as

$$\nu_q \equiv \left[\frac{\partial\,/\!/\,\bar{m}}{\partial\,/\!/\,\bar{q}_r}\right]_{p,T_1}$$
$$\mu_q \equiv \frac{1}{(\bar{T}_s - T_1)}\left[\frac{\partial \bar{T}_s}{\partial\,/\!/\,\bar{q}_r}\right]_{p,T_1} \quad \text{and} \quad \delta_q = \nu_q r - \mu_q k \tag{24}$$

For radiation-driven burning with volumetric absorption ($N_t \neq 0$ and ι_r = finite), only the limiting configuration of a very transparent condensed phase ($\iota_r << 1$) could be explicitly treated. Results were recently published by Son and Brewster,[27] and earlier by Kiskin,[25] extending a previous work[24] where the equivalence principle was assumed; details are given by Son in Chap. 6 of Ref. 28. In principle, the intrinsic burning stability region decreases. The general configuration of arbitrary ι_r is expected to lie in between the surface absorption boundary of Eq. (22) and the volumetric absorption boundary in the limit of very transparent condensed phase determined as

$$r > \frac{(k-1)^2}{(1-2\bar{q}_r)k + 1} \tag{25}$$

The results found by the FM and ZN methods are compared in Fig. 2, where the boundaries obtained from the nonlinear abstract approach are seen to exactly overlap with the ZN boundaries (reported with their original nomenclature). The additional intrinsic stability region (dashed area) revealed by the nonlinear abstract approach in the area below the line $a = b$, equivalent to $r > 1$ in the ZN plot, corresponds to a physical configuration neglected in the ZN analysis because it was considered unlikely to occur.

V. Linear Frequency Response Function

Another way to assess intrinsic stability of a combustion configuration is to define the unbounded response limit of the associated frequency response function. First, a specific flame model needs to be implemented in order to deduce the wanted frequency response function. The common departure step for all FM stability studies consists of properly perturbing the energy equation in both the condensed and gas phase, and match them at the perturbed surface boundary condition; the ZN approach requires the energy equation to be explicitly written in the condensed phase only.

Fluctuations of burning rate, subsequent to an externally controlled fluctuation of the forcing term, are sought. The forcing term is a sinusoidal fluctuation with angular frequency ω of either pressure or (external) radiant flux. Pressure- and radiation-driven frequency response are complex functions respectively defined as

$$R_p \equiv m'/\bar{m}/p'/\bar{p} \quad \text{and} \quad R_q \equiv m'/\bar{m}/I_0'/\bar{I}_0 \tag{26}$$

A positive real part of the frequency response function implies an amplification of the forcing waves. The basic mathematical assumption of linear theories is that all time-dependent variables (. . .) can be expressed as the sum of a steady-state value and a small disturbance of the type $(\ldots)' \cdot e^{i\omega t}$, whose amplitude has to be determined, but is always much smaller than the steady-state counterpart.

A. Transient Flame Model

Over the years, a wealth of experimental information on solid propellant flame structure was independently collected in the Eastern and Western countries; good accounts were respectively compiled[37,38] and provide useful suggestions as to the most suitable flame structures for a range of operating configurations. Based on this experimental information, a mechanistic transient flame model was developed by this research group[39] for distributed or spacewise thick flames (broad chemical reactions zones in the Russian literature). Sharp or spacewise thin flames (narrow chemical reaction zones in the Russian literature) can also be treated if proper care is taken of the possibly associated delta functions. Results from all quasisteady transient flames models accepted in the literature can be recovered as special cases. For distributed flames of thickness x_f featuring the maximum heat release rate just at the burning surface, the nonlinear heat feedback from the gas phase is obtained from Eq. (9) as

$$\tilde{q}_{g,s}(p, m) = mQ_g[(\gamma + 1)/\zeta_f]F(\gamma, \zeta_f) \tag{27}$$

being $\zeta_f = mc_g/k_g x_f \equiv m^2\langle t_g^\dagger\rangle$ a nondimensional quantity evaluated at the flame front, and $\langle t_g^\dagger\rangle$ an average characteristic time parameter of the gas phase to be defined for each flame model. The parameter γ is used to describe the space elongation of the flame (for details, see Ref. 39, p. 537). Notice that $\gamma = 0$ recovers the classical KTSS distributed flame, while the $\gamma > 0$ case deals with distributed flames of larger thickness. With the additional assumption of ζ_f large, find the following linearized expressions for the function $F(\gamma, \zeta_f)$: $F(\gamma = 0, \zeta_f$ large$) \equiv 1$ (i.e., the standard KTSS linear flame) and $F(\gamma = 1, \zeta_f$ large$) \equiv 1 - 1/\zeta_f$.

In this work, analytical solutions are provided for $\gamma = 0$ or $\gamma = 1$; the associated linear heat feedback is

$$\tilde{q}_{g,s}(p, m) = mQ_g[(\gamma + 1)/\zeta_f][1 - (\gamma/\zeta_f)] \tag{28}$$

The transient flame temperature is provided by a gas phase energy balance for any quasisteady flame as

$$T_f(t) = T_s(t) + \frac{Q_g(p) - \tilde{q}_{g,s}(p, m)/m(t)}{c_g} \tag{29}$$

The (average) characteristic gas phase time parameter is written as

$$\langle t_g^\dagger(p, m)\rangle \equiv f(p)g(m) \tag{30}$$

where the function $f(p)$, depending on pressure only, is evaluated under steady operations, but in the spirit of gas-phase quasisteadiness is assumed valid under transient conditions as well. The function $g(m)$ depends primarily on temperature and requires a specific submodel; notice that for convenience, in the sense of gas phase quasisteadiness, reference is made to the variable m, the instantaneous mass burning rate. For $\gamma = 0$ and $g(m) = 1$, the standard KTSS linear transient flame model is recovered. In all developments of this article,

only $g(m) = 1$ is considered; results for $g(m) \neq 1$ were reported in Ref. 40, for example.

B. Standard "Two-Parameter" Form

All QSHOD frequency response functions, for both FM and ZN methods, can be cast in the standard two-parameter form.[19] From a formal viewpoint, it is seen that two "universal" laws, respectively, for pressure and radiation-driven frequency response functions can be established.[26,40-42] Only parameter B (essentially related to the flame description) takes different values for different configurations; parameter A (related to surface pyrolysis) is not affected being defined in general as

$$A(p, I_0) \equiv \left[(\bar{T}_s - T_1) \frac{\partial /\!\!/ \bar{m}_s}{\partial \bar{T}_s} \right]_{p, I_0}$$

$$= \frac{\bar{E}_s}{\mathcal{R} \bar{T}_s} \frac{\bar{T}_s - T_1}{\bar{T}_s} = w_s(p, I_0) \tag{31}$$

C. Pressure-Driven Frequency Response

For pressure fluctuations, a general expressions is

$$R_p(\omega) = \frac{nAB_p + n_s(\lambda_1 - 1)}{\lambda_1 + (A/\lambda_1) - (1 + A) + AB_p} \tag{32}$$

whose static limit is

$$\lim_{\omega \to 0} R_p(\omega) = \lim_{\omega \to 0} \frac{m'/\bar{m}}{p'/\bar{p}} = n \tag{33}$$

being n defined by the experimental steady-state burning rate law.

For pressure-driven sharp flames, find

$$B_p \equiv (C_6 + c_g/c_c)/A \tag{34}$$

valid for arbitrary n_s if the following constraint is simultaneously satisfied:

$$n \left(C_6 + \frac{c_g}{c_c} \right) = \frac{c_g}{c_c} \left(\frac{E_s}{C_3} \frac{\beta_g}{2} - n_s \frac{C_1}{C_3} \right) \tag{35}$$

where

$$C_1 \equiv \frac{1}{2} \frac{c_g \bar{T}_s}{Q_g - c_g(\bar{T}_f - \bar{T}_s)}$$

$$C_3 \equiv \frac{\alpha_g + E_g}{2} \frac{\bar{T}_s}{\bar{T}_f} - \frac{1}{2} \frac{c_g \bar{T}_s}{Q_g - c_g(\bar{T}_f - \bar{T}_s)} \tag{36}$$

$$C_6 \equiv \frac{c_g}{c_c} \frac{1}{C_3} \left(E_s - \frac{\alpha_g + E_g}{2} \frac{\bar{T}_s}{\bar{T}_f} \right)$$

For pressure-driven distributed flames ($\gamma = 0$ and $\gamma = 1$) with arbitrary n_s, find

$$B_p = B_p(\gamma) \equiv \frac{1}{n} \left[W_p(\gamma) + \frac{c_g}{c_c} \frac{n_s}{A} \right] \tag{37}$$

$$W_p(\gamma) \equiv n \left[2(\gamma + 1) \left(1 - \frac{2\gamma}{\bar{\zeta}_f} \right) \frac{H_g}{\bar{\zeta}_f} + \frac{c_g}{c_c} \frac{1 - n_s/n}{A} \right] \tag{38}$$

where both parameters are convenient generalizations of the corresponding quantities

$$B \equiv \frac{1}{n} \left[W_p + \frac{c_g}{c_c} \frac{n_s}{A} \right] \tag{39}$$

$$W_p \equiv n \left[2(1 - \bar{H}_s) + \frac{c_g}{c_c} \frac{1 - n_s/n}{w_s} \right] \tag{40}$$

previously introduced by Culick (p. 26 of Ref. 21). The results by KTSS[22] are recovered by using B_p from Eq. (39) with $c_g/c_c = 1$.

For pressure-driven fluctuations in the ZN framework, as reformulated by Son and Brewster,[26] find

$$A \equiv k/r, \qquad B \equiv 1/k, \qquad n = \nu \quad \text{and} \quad n_s \equiv \delta/r \tag{41}$$

D. Radiation-Driven Frequency Response

For radiation fluctuations, a general expression is

$$R_q(\omega) = \frac{n_q AB_q \dfrac{(1 - N_t)(1 - \lambda_1) - \iota_r}{1 - \lambda_1 - \iota_r}}{\lambda_1 + \dfrac{A}{\lambda_1} - (1 + A) + AB_q - n_q AB_q \dfrac{N_t(1 - \lambda_1)}{\lambda_1(1 - \lambda_1 - \iota_r)}} \tag{42}$$

whose static limit is

$$\lim_{\omega \to 0} R_q(\omega) = \lim_{\omega \to 0} \frac{m'/\bar{m}}{I_0'/\bar{I}_0} = n_q \tag{43}$$

being n_q, defined by the experimental steady-state burning rate law.

For radiation-driven sharp flames, with arbitrary n_s within the constraint of Eq. (35), find

$$B_q \equiv \frac{C_6 + c_g/c_c}{A} + \bar{q}_r \quad \text{and} \quad n_q \equiv \frac{\bar{q}_r}{B_q} \tag{44}$$

For radiation-driven distributed flames ($\gamma = 0$ and $\gamma = 1$) with arbitrary n_s, find

$$B_q = B_q(\gamma) \equiv B_p(\gamma) + \bar{q}_r = \frac{1}{n} \left[W_p(\gamma) + \frac{c_g}{c_c} \frac{n_s}{A} \right] + \bar{q}_r$$

$$n_q \equiv \frac{\bar{q}_r}{B_q(\gamma)} \tag{45}$$

For radiation-driven fluctuations in the ZN framework, as reformulated by Son and Brewster,[26] find

$$A \equiv k/r, \qquad B \equiv 1/k, \qquad n_q \equiv \nu_q \quad \text{and} \quad n_s \equiv \delta_q/r \tag{46}$$

E. Unbounded Response Limit

By putting the denominator of $R_p = 0$ in Eq. (32), a complex equation is obtained. This defines QSHOD stability boundaries and the related frequency laws for pressure-driven linear burning for both FM and ZN approaches. These boundaries correspond to the condition of unbounded response of the burning propellant even for vanishing fluctuations of the forcing term and were first identified by Denison and Baum[17] for a sharp flame subjected to pressure fluctuations. In the FM approach the stability boundary is

$$A = K(K - 1)/2 \tag{47}$$

while the frequency of the unbounded response is given by

$$\Omega = [(K - 1)/2]\sqrt{K(K - 2)} \tag{48}$$

requiring $K > 2$ for real Ω. These results are valid for both sharp and distributed flames, since for both configurations

$$K = 1 + A - AB_p \tag{49}$$

but the explicit expressions of K are different because the proper value of B_p has to be introduced [see Eq. (34) for sharp flames and Eq. (37) for distributed flames]; detailed relationships are reported.[40] Comparison of these results with those obtained from the formal FM and ZN stability analyses is discussed in the next section.

Putting the denominator of $R_q = 0$ in Eq. (42), yields QSHOD stability boundaries and the related frequency laws for radiation-driven linear burning. Exactly the same formal results are obtained if surface absorption is assumed for the radiation-driven frequency response; but relevant parameters implicitly depend on the radiant flux intensity as well. For pressure fluctuations or radiation fluctuations in the limit of surface absorption, the same set of equations holds true; in the FM approach Eqs. (47–49) are true if B_q replaces B_p in Eq. (49).

For radiation-driven frequency response with volumetric absorption ($N_t \neq 0$ and ι_r = finite), only the limiting configuration of a very transparent condensed phase ($\iota_r << 1$) can be explicitly treated. By extending the previous analysis, the expression of K [Eq. (49)] and frequency of the unbounded response [Eq. (48)] are found to be unaffected, while the stability boundary is now given by

$$A(1 - N_t\bar{q}_r) = K(K - 1)/2 \tag{50}$$

Thus, the intrinsic burning stability region decreases. This finding extends the corresponding previous result by just incorporating the factor $(1 - N_t\bar{q}_r)$, which collapses to 1 under pressure-driven ($\bar{q}_r = 0$) or radiation-driven burning in the limit of surface absorption ($N_t = 0$).

VI. General Comparison of QSHOD Intrinsic Stability for Inert Condensed Phase

For the reader's convenience, first recall that in their classical analysis of premixed flames Denison and Baum[17] introduced three parameters (A_{DB}, α_{DB}, and q_{DB}) and formulated the instability condition for a steady-state burning propellant as

$$q_{DB} > 1 \tag{51}$$

$$q_{DB}^2 - q_{DB} - 2A_{DB} > 0 \tag{52}$$

exactly matching the ZN stability conditions (see also p. 623 of Ref. 13). Similar results for diffusion flames were found later by KTSS,[22] again using three parameters (w_s, B_{KTSS}, and A_{KTSS}). A full discussion is reported by Williams[43]; see in particular pp. 330–335.

In the linear regime, a complete agreement is found between the abstract nonlinear stability analysis (here performed within the FM framework), unbounded response limit of pressure- or radiation-driven frequency responses (available for both the FM and ZN frameworks), and the ZN stability analysis. A formal equivalence is obtained if one puts

$$\begin{aligned} A &= A_{DB} = w_s = a = k/r \\ B_q &= \alpha_{DB} = B_{KTSS} = (1 + A - K)/A \\ &= (1 + a - b)/a = 1/k \end{aligned} \tag{53}$$

$$K = q_{DB} = A_{KTSS} = 1 + A - AB_q = 1 + (k/r) - (1/r) \tag{54}$$

where, in general, all parameters are both pressure- and radiation-dependent. The positions in Eqs. (53) and (54) make all the relationships reported above for the stability boundary and oscillation frequency equivalent and interchangeable. Therefore, all methods (each within its validity limits) yield the same intrinsic stability boundary as, e.g.,

$$a = b(b - 1)/2 \tag{55}$$

and the same frequency of the oscillatory solution just at the stability boundary as, e.g.,

$$\Omega = [(b - 1)/2]\sqrt{b(b - 2)}$$

The last result about the frequency of unbounded response recovers in particular the classical prediction $\Omega = A\sqrt{B}$ by Culick (p. 2251 of Ref. 19).

Thus, allowing either infinitesimal (linear theories) or small but finite disturbances (nonlinear theories), yield the same intrinsic stability boundaries and frequencies. A summarizing overview of intrinsic burning stability in the broad QSHOD framework is shown in Fig. 2. Typical trends, computed with a standard set of properties for both an homogeneous noncatalyzed double-base (DBN) and composite ammonium perchlorate-(AP)-based propellants of national production (see Table 1), are illustrated in Fig. 3. The higher value of a clearly reveals the more vigorous gasification of the AP-based composition with larger oxidizer content. The intrinsic stability features of all compositions are well inside the $r = 1$ limit set in the ZN stability analysis, as indicated in the figure. A somewhat unexpected effect of radiation driven burning on intrinsic stability is emphasized in Fig. 4: while large radiant flux are always stabilizing (forcing the deflagration wave to saturate into an ablation wave), moderate values can trigger instability (due to flame elongation). Notice that burning configurations unstable under adiabatic burning (at subatmospheric pressure) are made stable by large enough radiant flux, but also marginally stable burning configurations (just at atmospheric pressure) are first destabilized and then made stable by large enough radiant flux. The plot in Fig. 4 was purposely obtained with a convenient value of surface heat release (Q_s = 136 cal/g) to underline some peculiarities of radiation-assisted burning. The expectations of Fig. 3 and Fig. 4 were confirmed by numerical computations in terms of boundary location and oscillatory frequency.

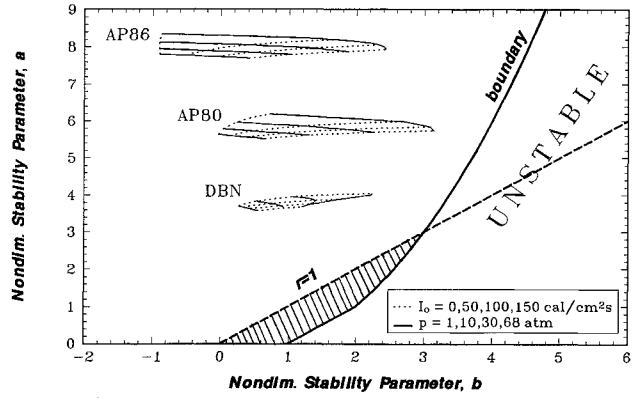

Fig. 3 Intrinsic stability features of DBN and AP-based solid propellants.

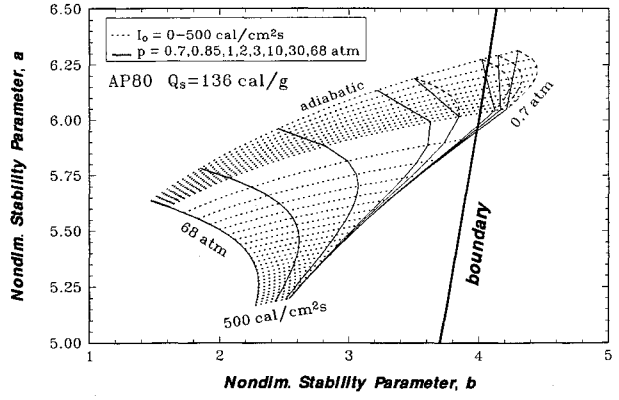

Fig. 4 Intrinsic stability features of radiation assisted burning.

Table 1 Properties of composite solid propellant AP.PBAA/80.20 used as test case

Assumed or measured properties	Computed properties	Reference properties at 68 atm
AP mass fraction, $ox = 80\%$ Condensed phase density, $\rho_c = 1.54$ g/cm^3 Condensed phase specific heat, $c_c = 0.33$ cal/g Condensed phase thermal diffusivity, $\alpha_c = 1.400E - 03$ cm^2/s Initial temperature of sample, $T_1 = 300$ K AP crystalline transition temperature, $T_{tra} = 513$ K Condensed phase absorption coefficient, $\tilde{\alpha}_\lambda = 1000$ cm^{-1} Surface activation energy, $\tilde{E}_s = 1.600E + 04$ cal/mole Pyrolysis law pressure power, $n_s = 0$ Pyrolysis law temperature power, $\alpha_s = 0$ Gas phase activation energy, $\tilde{E}_g = 2.000E + 04$ cal/mole Gas phase specific heat, $c_g = 0.33$ cal/g K Gas phase thermal conductivity, $k_g = 2.000E - 04$ cal/cm s K Average molecular mass of gas products, $\bar{M} = 26$ g/mole $\alpha\beta\gamma$ flame model parameters: $\alpha(p) = 0$, $\beta(p) = 1$, $\gamma(p) = 1$ Steady burning rate, $\bar{r}_b = 0.837(\bar{p}/p_{ref})^{0.46}$ Steady surface heat release (positive if exothermic), $\bar{Q}_s = 100$ Steady burning surface temperature, $\bar{T}_s = 1000(\bar{p}/p_{ref})^{0.053}$ Steady adiabatic flame temperature, $\bar{T}_f = 2430(\bar{p}/p_{ref})^{0.01}$	Condensed phase thermal conductivity, $k_c = 7.115E - 03$ cal/cm s K Condensed phase thermal responsivity, $\Gamma_c = 1.902E - 02$ cal/cm^2 $\sqrt{\text{s}}$ K	Pressure, $p_{ref} = 68$ atm Temperature, $T_{ref} = 300$ K Condensed phase characteristic length, $\alpha_c/r_{b,ref} = 16.73$ μm Condensed phase characteristic time, $\alpha_c/r^2_{b,ref} = 1.998$ ms Condensed phase sink, $Q_{ref} = 231.0$ cal/g Gas phase heat release, $Q_{g,ref} = 544.7$ cal/g Flame thickness, $x_{f,ref} = 65.31$ μm Thermal flux, $\bar{q}_{ref} = 297.8$ cal/cm^2 s

VII. Effects of a Uniform Heat Release Rate in the Condensed Phase

Frequency response functions were also obtained in the more general configuration of heat release distribution volumetrically distributed in the condensed phase. Unfortunately, the problem is by far too complex for a general treatment, and thus, only the special case of zero-order reaction with uniform heat release rate distribution is discussed. It is assumed that a further source term of the kind $Q_c\tilde{\varepsilon}_c/c_c$ is present in Eq. (1) over a layer of thickness l_c, that is for $0 < x < x_l$ or $T_s > T > T_l$, being T_l a known property of the propellant under test. Comparison with the standard surface concentrated chemical reactions is carried out by keeping constant the total amount $Q_x = Q_c + Q_s$ of heat release in the condensed phase, that is by volumetrically distributing over the condensed-phase different fractions Q_c of the total Q_x. Steady-state mass conservation requires

$$\bar{m} = \int_{-\bar{l}_c}^{0-} \rho_c \tilde{\varepsilon}_c \, dx \tag{56}$$

By matching the thermal profiles at both the burning surface and edge of the reacting layer in the condensed phase, the steady-state thermal profiles can be obtained[18,29]; see also the pertinent comments in Ref. 44.

A distributed or spacewise thick flames of thickness x_f are assumed for the gas phase. Thus, the heat feedback from the gas phase is given by Eq. (27) and the (average) characteristic gas phase time parameter by Eq. (30). A difference arises when evaluating the function $f(p)$ through the steady-state adiabatic energy balance at the burning surface[45]

$$f(p) = \frac{1}{\bar{m}^2}\frac{\gamma+1}{2}\frac{H_g}{1-H_c-\bar{H}_s} \times \left(1+\sqrt{1+4\frac{\gamma}{\gamma+1}\frac{1-H_c-\bar{H}_s}{H_g}}\right) \tag{57}$$

including as particular case the inert condensed phase configuration. The standard KTSS linear transient flame model is recovered for $\gamma = 0$ and $Q_c = H_c = 0$.

By repeating the standard linear perturbation approach, the externally driven frequency response functions can be obtained. While l_c and $\tilde{\varepsilon}_c$ are fluctuating quantities, it is assumed that Q_c and Q_g are not fluctuating.

A. Frequency Response Functions

For pressure-driven distributed flames ($\gamma = 0$ and $\gamma = 1$) with arbitrary n_s, find

$$R_p(\omega) = \frac{nAB_p + n_s(\Lambda_1 - 1)}{\Lambda_1 - (A/\lambda_1\lambda_2)(\Lambda_1 D_1 - D_2) - (1+A) + AB_p} \tag{58}$$

whose static limit is

$$\lim_{\omega\to 0} R_p(\omega) = \lim_{\omega\to 0}\frac{m'/\bar{m}}{p'/\bar{p}} = n \tag{59}$$

Notice that

$$\Lambda_1 \equiv \frac{\lambda_1 + \lambda_2 D_3}{1+D_3} \to \lambda_1 \quad \text{for} \quad Q_c \to 0 \tag{60}$$

$$(A/\lambda_1\lambda_2)(\Lambda_1 D_1 - D_2) \to -(A/\lambda_1) \quad \text{for} \quad Q_c \to 0 \tag{61}$$

being D_1, D_2, and D_3 computable quantities.

In the previous expression for the pressure-driven frequency response function

$$B_p = B_p(\gamma) \equiv (1/n)[W_p(\gamma) + (c_g/c_c)(n_s/A)] \tag{62}$$

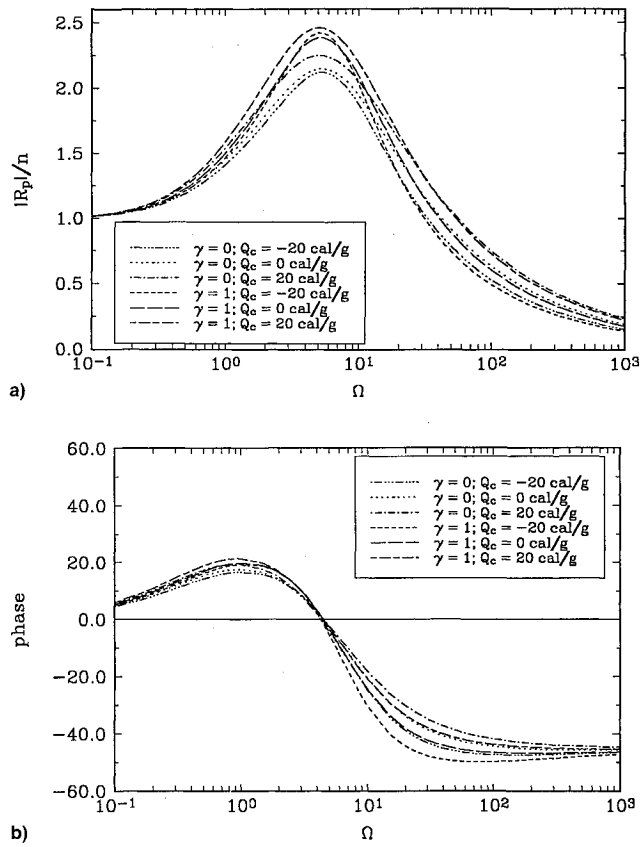

Fig. 5 a) Magnitude and b) phase of normalized pressure-driven frequency response function of distributed flames at 1 atm for $\gamma = 0$ or $\gamma = 1$ and the indicated values of condensed phase heat release.

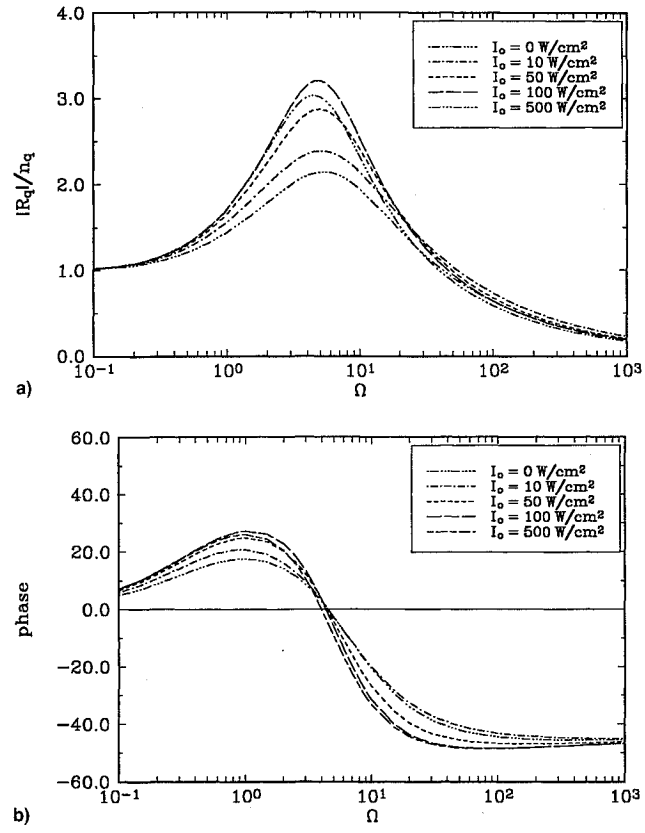

Fig. 7 a) Magnitude and b) phase of normalized radiation driven frequency response function of distributed flames for $\gamma = 0$, $p = 1$ atm, $Q_c = 20$ cal/g, and $Q_s = 80$ cal/g, and the indicated values of radiant heat flux.

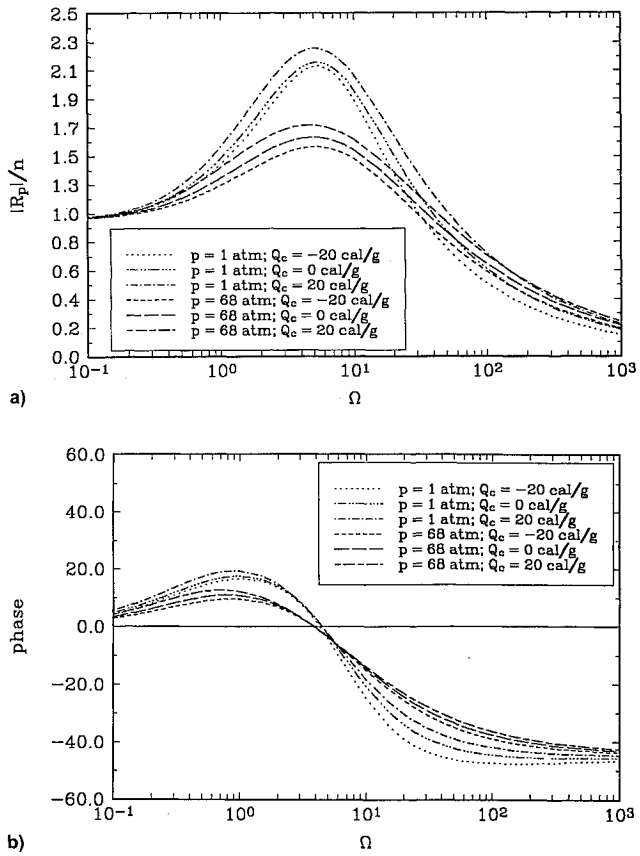

Fig. 6 a) Magnitude and b) phase of normalized pressure driven frequency response function of distributed flames for $\gamma = 0$, $p = 1$, or 68 atm, and the indicated values of condensed phase heat release.

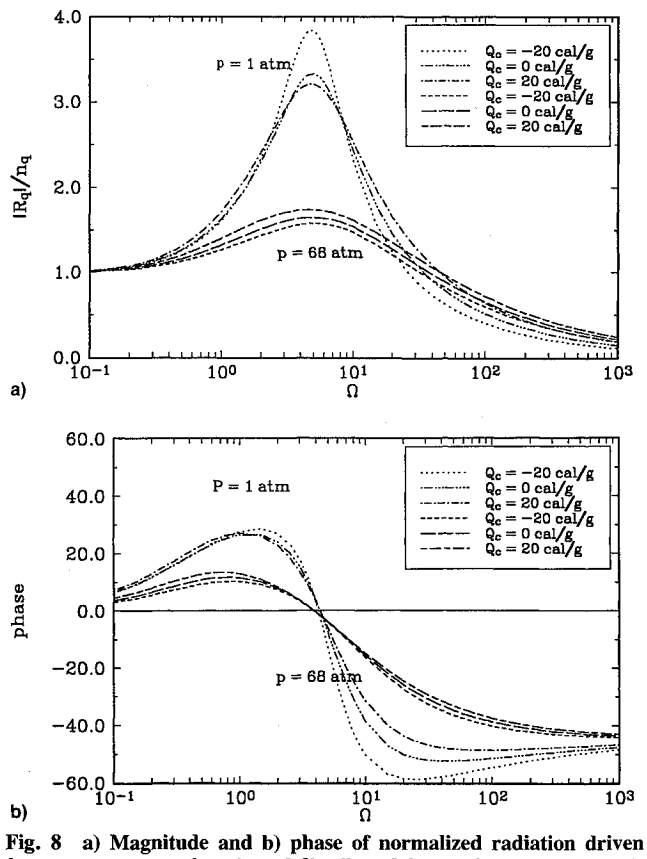

Fig. 8 a) Magnitude and b) phase of normalized radiation driven frequency response function of distributed flames for $\gamma = 0$, $p = 1$, and 68 atm, $I_0 = 100$ W/cm², and the indicated values of condensed phase heat release.

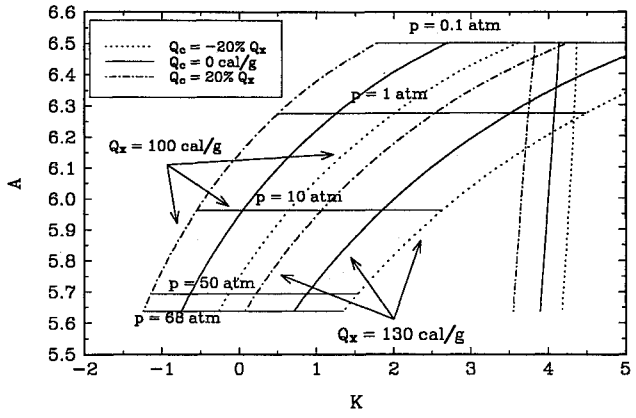

Fig. 9 Intrinsic stability map of the test case, under adiabatic burning, for $\gamma = 0$ and the indicated values of the operating conditions.

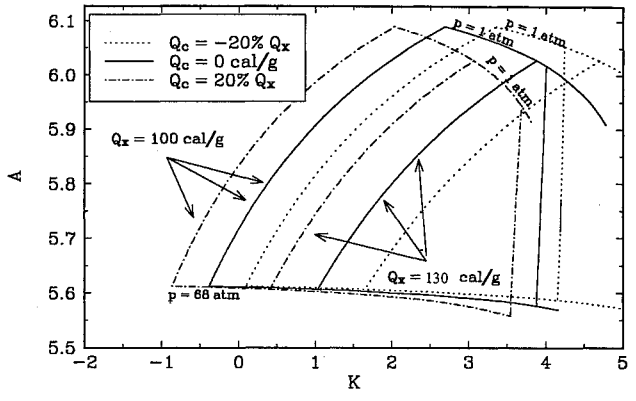

Fig. 10 Intrinsic stability map of the test case, under radiation assisted burning with $I_0 = 100$ W/cm², for $\gamma = 0$ and the indicated values of the operating conditions.

$$W_p(\gamma) \equiv \frac{H_g}{\bar{\zeta}_f}\left[1 + \frac{\dfrac{(1+\Lambda_{11})(1-H_c) - 2\bar{H}_s}{2(1-H_c-\bar{H}_s)}\left(1 + \sqrt{1 + 4\dfrac{\gamma}{\gamma+1}\dfrac{1-H_c-\bar{H}_s}{H_g}}\right) - 1}{\sqrt{1 + 4\dfrac{\gamma}{\gamma+1}\dfrac{1-H_c-\bar{H}_s}{H_g}}}\right]$$

$$+ n\frac{(\Lambda_{10}-1) + \dfrac{c_g}{c_c}}{\sqrt{1 + 4\dfrac{\gamma}{\gamma+1}\dfrac{1-H_c-\bar{H}_s}{H_g}}}\frac{1-\dfrac{n_s}{n}}{(\gamma+1)A} \tag{63}$$

are both further generalizations, respectively, of Eqs. (39) and (40) previously recalled.

Typical trends are illustrated in Fig. 5, showing the effect of flame thickness, and Fig. 6, showing the effect of pressure, for the indicated set of operating conditions. Both endothermic and exothermic reactions were tested; the total heat release $Q_x = Q_s + Q_c$ is kept constant. The results of Fig. 5 confirm that thickening of flames is destablizing, while the results of Fig. 6 confirm that increasing pressure is stabilizing. Stability assessments are presented in what follows.

For radiation-driven distributed flames ($\gamma = 0$ and $\gamma = 1$) with arbitrary n_s, find

$$R_q(\omega) = \frac{n_q A B_q(1 - N_t - \Lambda_3)}{\Lambda_1 + (A/\lambda_1\lambda_2)(\Lambda_1 D_1 - D_2) - (1+A) + AB_q - n_q AB_q(\iota_r\Lambda_3/\lambda_1\lambda_2)} \tag{64}$$

where

$$\Lambda_3 = \left[\frac{\lambda_1 + \lambda_2 D_3}{1+D_3}\left(D_4 + \frac{1}{\iota_r^2 - \iota_r + \lambda_1\lambda_2}\right) - \lambda_2 D_4 - \frac{\iota_r}{\iota_r^2 - \iota_r + \lambda_1\lambda_2}\right] N_t(1 - \bar{\bar{r}}_\lambda)\iota_r \exp(-\bar{\bar{a}}_\lambda \bar{l}_c) \tag{65}$$

being D_4 a computable quantity.

Typical trends are illustrated in Fig. 7, showing the effect of average radiant flux intensity for $Q_c = 20$ cal/g, and Fig. 8, showing the effect of pressure, for the indicated set of operating conditions. The results of Fig. 7 confirm the inversion effect due to large radiant flux, while the results of Fig. 8 confirm that increasing pressure squeezes the radiation effect.

B. Unbounded Response Limit

By putting the denominator of $R_p = 0$ in Eq. (58), yields the QSHOD stability boundaries and the related frequency laws for pressure-driven linear burning with chemically reacting condensed phase. Since analytical treatments are now forbidden, a numerical approach was implemented to get the solution of the complex equation. The results obtained are reported in Fig. 9 (adiabatic burning) and Fig. 10 (radiation-assisted burning) for the indicated values of operating conditions, and in particular, of the heat release partition between condensed phase Q_c and burning surface Q_s. The plane A vs $K = 1 + A - AB_q$ was selected as representative because it permits to easily verify whether the chemically inert condensed phase results are recovered. On this plane, different unbounded response limits are found for different values of Q_c; for $Q_c = 0$, the standard QSHOD limit for inert chemically inert condensed phase is always recovered. The previous trends are again verified: decreasing pressure is destabilizing, while increasing total condensed phase heat release $Q_x = Q_s + Q_c$ is destabilizing. In addition, observe that chemical reactions passing from endothermic to exothermic imply a stabilizing effect; e.g., contrast at 1 atm and $Q_x = 130$ cal/g the time-invariant steady solution for $Q_c = -20\%\ Q_x$ (linearly unstable) with the time-invariant steady solution for $Q_c = +20\%Q_x$ (linearly stable). For decreasing pressure, e.g., at 0.1 atm, the whole investigated Q_c range is linearly unstable; for increasing pressure, e.g., at 10 atm, the whole investigated Q_c range is linearly stable. But under all investigated circumstances, the locus of steady solutions with endothermic heat release is systematically closer to the unbounded response limit, especially for large total heat release Q_x. Similar trends are observed in Fig. 10 for the investigated set of parameters.

VIII. Conclusions and Future Work

All QSHOD intrinsic stability analyses for chemically inert condensed phase predict the same intrinsic stability boundary. The two commonly used approaches known as FM and ZN are equivalent. The results obtained from a nonlinear abstract analysis of intrinsic burning stability confirm and somewhat extend the classical ZN stability plot. For all stability analyses, steady-state solutions are expected to be time-invariant on the left of the stability boundary and oscillatory just on the boundary. The predicted frequencies of the unbounded response (frequency-response functions) or self-sustained oscillatory burning (stability theories) just on the boundary are identical. The boundary means incipient instability of the time-invariant solution and beginning of Hopf bifurcation.

Frequency-response functions and unbounded response limits were also obtained for volumetrically distributed chemical reactions in the condensed phase with a uniform heat release rate distribution. Both endothermic and exothermic reactions are allowed. The results of chemically inert condensed phase are recovered as a particular case. The stabilizing effects of large pressures, short flames, and/or low total heat release in the condensed phase are confirmed; in addition, endothermic reactions are found to promote instability.

Fundamental progress is needed as to the structure as well as planarity of surface layer, and chemical as well as radiative processes of condensed phase especially if heterogeneous. This, in turn, calls also for sophisticated nonintrusive diagnostic techniques and multidimensional computational capabilities. Work in this area is presently under progress.

Acknowledgments

The authors gratefully acknowledge the financial support of MURST Quota 40% and the valuable discussions with C. D. Pagani and M. Verri during preparation of this manuscript.

References

[1]Zeldovich, Ya. B., "On the Combustion Theory of Powders and Explosives," *Journal of Experimental and Theoretical Physics*, Vol. 12, 1942, pp. 498–510.

[2]Zeldovich, Ya. B., Leypunskii, O. I., and Librovich, V. B., *The Theory of the Unsteady Combustion of Powder*, Nauka, Moscow, Russia, 1975.

[3]Mathes, H. B., "Applications of Combustion Stability Technology to Solid Propellant Rocket Motors," *Nonsteady Burning and Combustion Stability of Solid Propellants*, edited by L. DeLuca, E. W. Price, and M. Summerfield, Vol. 143, Progress in Astronautics and Aeronautics, AIAA, Washington, DC, 1992, pp. 781–804, Chap. 19.

[4]Strand, L. D., and Brown, R. S., "Laboratory Test Methods for Combustion Stability Properties of Solid Propellants," *Nonsteady Burning and Combustion Stability of Solid Propellants*, edited by L. DeLuca, E. W. Price, and M. Summerfield, Vol. 143, Progress in Astronautics and Aeronautics, AIAA, Washington, DC, 1992, pp. 689–718, Chap. 17.

[5]Mihlfeith, C. M., Baer, A. D., and Ryan, N. W., "The Response of a Burning Propellant Surface to Thermal Radiation," *AIAA Journal*, Vol. 10, No. 10, 1972, pp. 1280–1285.

[6]Ibiricu, M. M., and Williams, F. A., "Influence of Externally Applied Thermal Radiation on the Burning Rates of Homogeneous Solid Propellants," *Combustion and Flame*, Vol. 24, 1975, pp. 185–198.

[7]T'ien, J. S., "Oscillatory Burning of Solid Propellant Including Gas Phase Time Lag," *Combustion Science and Technology*, Vol. 5, No. 2, 1972, pp. 47–54.

[8]Novozhilov, B. V., *Nonstationary Combustion of Solid Rocket Fuels*, Translation AFSC FTD-MT-24-317-74, 1973, Nauka, Moscow, Russia.

[9]Novozhilov, B. V., "The Theory of Nonstationary Condensed Propellant Burning Allowing for the Time Lag," *Soviet Journal of Chemical Physics*, Vol. 7, No. 5, 1988, pp. 674–687.

[10]Novozhilov, B. V., "Influence of Gas Phase Inertia on Stability of Propellant Burning," *Kimicheskaya Fizika*, Vol. 7, No. 3, 1988, pp. 388–396.

[11]Novozhilov, B. V., "Combustion of Volatile Condensed System at Oscillatory Pressure," *Kimicheskaya Fizika*, Vol. 8, No. 1, 1989, pp. 102–111.

[12]Novozhilov, B. V., "Acoustic Admittance of Condensed Phase Surface During Combustion," *Kimicheskaya Fizika*, Vol. 10, No. 11, 1991, pp. 1518–1532.

[13]Novozhilov, B. V., "Theory of Nonsteady Burning and Combustion Stability of Solid Propellants by the ZN Method," *Nonsteady Burning and Combustion Stability of Solid Propellants*, edited by L. DeLuca, E. W. Price, and M. Summerfield, Vol. 143, Progress in Astronautics and Aeronautics, AIAA, Washington, DC, 1992, pp. 601–641, Chap. 15.

[14]Margolis, S. B., and Williams, F. A, "Diffusional/Thermal Coupling and Intrinsic Instability of Solid Propellant Combustion," *Combustion Science and Technology*, Vol. 59, 1988, pp. 27–84.

[15]Margolis, S. B., and Williams, F. A, "Stability of Homogeneous Solid Deflagration with Two-Phase Flow in the Reaction Zone," *Combustion and Flame*, Vol. 79, 1990, pp. 199–213.

[16]Clavin, P., and Lazimi, D., "Theoretical Analysis of Oscillatory Burning of Homogeneous Solid Propellant Including Nonsteady Gas Phase Effects," *Combustion Science and Technology*, Vol. 83, 1992, pp. 1–32.

[17]Denison, M. R., and Baum, E., "A Simplified Model of Unstable Burning in Solid Propellants," *ARS Journal*, Vol. 31, 1961, pp. 1112–1122.

[18]Culick, F. E. C., "Calculation of the Admittance Function for a Burning Surface," *Astronautica Acta*, Vol. 13, No. 3, 1967, pp. 221–237.

[19]Culick, F. E. C., "A Review of Calculations for Unsteady Burning of a Solid Propellant," *AIAA Journal*, Vol. 6, No. 12, 1968, pp. 2241–2255.

[20]Culick, F. E. C., "An Elementary Calculation of the Combustion of Solid Propellants," *Astronautica Acta*, Vol. 14, No. 2, 1969, pp. 171–181.

[21]Culick, F. E. C., "Some Problems in t' Unsteady Burning of Solid Propellants," Naval Weapons Center, NWC TP 4668, China Lake, CA, 1969.

[22]Krier, H., T'ien, J. S., Sirignano, W. A., and Summerfield, M., "Nonsteady Burning Phenomena of Solid Propellants: Theory and Experiments," *AIAA Journal*, Vol. 6, No. 2, 1968, pp. 278–288; also Krier, H., "Solid Propellant Burning in Nonsteady Pressure Fields," Ph.D. Dissertation, Aerospace and Mechanical Sciences, Princeton Univ., Princeton, NJ, 1968.

[23]T'ien, J. S., "Theoretical Analysis of Combustion Instability," *Fundamentals of Solid Propellant Combustion*, edited by K. K. Kuo and M. Summerfield, Vol. 90, Progress in Astronautics and Aeronautics, AIAA, New York, 1984, pp. 791–840, Chap. 14.

[24]Assovskii, I. G., and Istratov, A. G., "Solid Propellant Combustion in the Presence of Photoirradiation," *Journal of Applied Mechanics and Technical Physics*, Vol. 12, No. 5, 1971, pp. 692–698.

[25]Kiskin, A. B., "Stability of Stationary Powder Combustion Acted on by a Constant Light Flux," *Combustion Explosion and Shock Waves*, Vol. 19, No. 3, 1983, pp. 295–297.

[26]Son, S. F., and Brewster, M. Q., "Linear Burning Rate Dynamics of Solids Subjected to Pressure or External Radiant Flux Oscillations," *Journal of Propulsion and Power*, Vol. 9, No. 2, 1993, pp. 222–232.

[27]Son, S. F., and Brewster, M. Q., "Unsteady Combustion of Solid Propellants Subjected to Dynamic External Radiant Heating," *Combustion Explosion and Shock Waves*, Vol. 29, No. 3, 1993, pp. 31–36.

[28]Son, S. F., "The Unsteady Combustion of Radiant Heat Flux Driven Energetic Solids," Ph.D. Dissertation, Univ. of Illinois at Urbana–Champaign, Urbana, IL, 1993.

[29]Lengellé, G., Kuentzmann, P., and Rendolet, C., "Response of a Solid Propellant to Pressure Oscillations," AIAA Paper 74-1209, Oct. 1974.

[30]Son, S. F., Burr, R. F., Brewster, M. Q., Finlinson, J. C., and Hanson-Parr, D., "Nonsteady Burning of Solid Propellants with an External Radiant Heat Flux: A Comparison of Models with Experiment," AIAA Paper 91-2194, June 1991.

[31]Merkle, C. L., Turk, S. L., and Summerfield, M., "Extinguishment of Solid Propellants by Rapid Depressurization," Princeton Univ., Aerospace and Mechanical Sciences Dept., Rept. 880, Princeton, NJ, 1969.

[32]Merkle, C. L., Turk, S. L., and Summerfield, M., "Extinguishment of Solid Propellant by Depressurization: Effects of Propellant Parameters," AIAA Paper 69-176, Jan. 1969.

[33]Henry, D., "Geometric Theory of Semilinear Parabolic Equations," *Lecture Notes in Mathematics*, Vol. 840, Springer–Verlag, New York, 1981.

[34]Brauner, C. M., Lunardi, A., and Schmidt-Lainé, C., "Stability of Traveling Waves with Interface Conditions," *Nonlinear Analysis*, Vol. 19, pp. 455–474, 1992.

[35]Pagani, C. D., and Verri, M., "Stability Analysis of the Travelling Wave Solutions in Burning Solid Propellants," First World Congress of Nonlinear Analysts, Tampa, FL, 1993.

[36]Pagani, C. D., and Verri, M., private communication, Dipartimento di Matematica, Politecnico di Milano, Milan, Italy, 1994.

[37]Zenin, A. A., "Thermophysics of Stable Combustion Waves of Solid Propellants," *Nonsteady Burning and Combustion Stability of Solid Propellants*, edited by L. DeLuca, E. W. Price, and M. Summerfield, Vol. 143, Progress in Astronautics and Aeronautics, AIAA, Washington, DC, 1992, pp. 197–231, Chap. 6.

[38]Kubota, N., "Flame Structure of Modern Solid Propellants," *Nonsteady Burning and Combustion Stability of Solid Propellants*, edited by L. DeLuca, E. W. Price, and M. Summerfield, Vol. 143, Progress in Astronautics and Aeronautics, AIAA, Washington, DC, 1992, pp. 233–259, Chap. 7.

[39]DeLuca, L., "Theory of Nonsteady Burning and Combustion Stability of Solid Propellants by Flame Models," *Nonsteady Burning and Combustion Stability of Solid Propellants*, edited by L. DeLuca, E. W. Price, and M. Summerfield, Vol. 143, Progress in Astronautics and Aeronautics, AIAA, Washington, DC, 1992, pp. 519–600, Chap. 14.

[40]Cozzi, F., Cristiani, R., and DeLuca, L., "Stability of Radiation Driven Burning of Solid Rocket Propellants," 44th Congress of the International Astronautical Federation, IAF Paper 93-S.2.467, Graz, Austria, 1993.

[41]DeLuca, L., Pagani, C. D., and Verri, M., "A Review of Solid Rocket Propellant Combustion," 19th International Symposium on Space Technology and Science, ISTS Paper 94-a-30v, Yokohama, Japan, 1994.

[42]DeLuca, L., Cozzi, F., DiSilvestro, R., and Mazza, P., "Frequency Response Function of Radiation Driven Burning of Solid Rocket Propellants," 19th International Symposium on Space Technology and Science, ISTS Paper 94-a-26, Yokohama, Japan, 1994.

[43]Williams, F. A., *Combustion Theory*, 2nd ed., Benjamin/Cummings Publishing, Menlo Park, CA, 1985, Chaps. 7–9.

[44]Zeldovich, Ya. B., Barenblatt, G. I., Librovich, V. B., and Makhviladze, G. M., *The Mathematical Theory of Combustion and Explosions*, Plenum, New York, 1985, p. 106.

[45]DiSilvestro, R., "Risposta in Frequenza e Stabilitá di Combustione dei Propellenti Solidi," M.S. Thesis in Aeronautical Engineering, Politecnico di Milano, Milan, Italy, 1994.